Lymphocytic choriomeningitis virus Clone 13 infection causes either persistence or acute death dependent on IFN-1, cytotoxic T lymphocytes (CTLs), and host genetics

Michael B. A. Oldstone[a,1], Brian C. Ware[a], Lucy E. Horton[a], Megan J. Welch[a], Roberto Aiolfi[b], Alessandro Zarpellon[b], Zaverio M. Ruggeri[b], and Brian M. Sullivan[a]

[a]Department of Immunology and Microbiology, The Scripps Research Institute, La Jolla, CA 92037; and [b]Department of Molecular Medicine, Medolago Ruggeri (MERU) Foundation–Roon Research Center for Vascular Biology, The Scripps Research Institute, La Jolla, CA 92037

Contributed by Michael B. A. Oldstone, June 15, 2018 (sent for review March 19, 2018; reviewed by Ralph S. Baric and Allan J. Zajac)

Understanding of T cell exhaustion and successful therapy to restore T cell function was first described using Clone (Cl) 13 variant selected from the lymphocytic choriomeningitis virus (LCMV) Armstrong (ARM) 53b parental strain. T cell exhaustion plays a pivotal role in both persistent infections and cancers of mice and humans. C57BL/6, BALB, SWR/J, A/J, 129, C3H, and all but one collaborative cross (CC) mouse strain following Cl 13 infection have immunosuppressed T cell responses, high PD-1, and viral titers leading to persistent infection and normal life spans. In contrast, the profile of FVB/N, NZB, PL/J, SL/J, and CC NZO mice challenged with Cl 13 is a robust T cell response, high titers of virus, PD-1, and Lag3 markers on T cells. These mice all die 7 to 9 d after Cl 13 infection. Death is due to enhanced pulmonary endothelial vascular permeability, pulmonary edema, collapse of alveolar air spaces, and respiratory failure. Pathogenesis involves abundant levels of Cl 13 receptor alpha-dystroglycan on endothelial cells, with high viral replication in such cells leading to immunopathologic injury. Death is aborted by blockade of interferon-1 (IFN-1) signaling or deletion of CD8 T cells.

persistence | vascular permeability | death | platelet aggregation

T cell exhaustion is the cardinal event by which persistent viral infections and many cancers pivot (1–3). T cell exhaustion (4, 5), the role for reconstituting functional T cells (6, 7), negative immune regulators (NIRs) in causation, and NIRs removal to restore T cell function (1–3, 8–13) were initially discovered and defined from studies of lymphocytic choriomeningitis virus (LCMV) Clone 13 (Cl 13) infection of C57BL/6 (B6) mice (5, 8–12). Findings uncovered by Cl 13 infection of mice were subsequently shown to occur in humans with persistent viral infections and with several cancers (2, 14–16). While immunotherapy to block NIRs and restore T cell function in vivo was effective for those defined inbred strains of mice studied, by comparison, restoration of T cell function was only partially effective for humans, ranging from 70% for melanoma and non-small cell lung cancer to 20% for renal cell carcinoma. Similar treatments in vitro to block NIRs and restore T cell functions in persistent viral infections of humans were effective, but less so than corresponding in vitro or in vivo therapeutic approaches for persistent viral infections of the few genetically defined mice studied. To begin to resolve this conundrum, we initiated studies using a broad number of inbred mouse strains and the collection of Collaborative Cross (CC) founder mice (17–19). CC founder mice and their crosses are now available for mapping of the mouse genome. Our initial intent was to provide a foundation necessary to identify distinct genetic loci and genes that control T cell exhaustion on one hand and a vigorous T cell response on the other. The intended long-range goal was to identify genes or genetic markers in mice that may relate to differences where T cell exhaustion does or does not occur in humans to help explain different responses observed in treatment of cancers, persistent infections, or autoimmune diseases (20). These studies would complement other ongoing mapping studies of outbred human population in which immunotherapy to block NIRs failed to restore T cell function.

Here, we report on dramatically different responses following Cl 13 infection in both genetically defined routine inbred mouse strains and CC founder mice. Several inbred mouse strains (C57BL/6, BALB/c, SWR/J, C3H/HeJ) and seven of eight CC founder mouse strains (C57BL/6, A/J, 129S1Sv/ImJ, NOD/LtJ, CAST/EiJ, PWK/PhJ, and WSB/EiJ), when given Cl 13, generated low cytotoxic T lymphocyte (CTL) activity, high PD-1 levels, high viral titers, and usually low to moderate type 1 IFN levels and became persistently infected. In sharp contrast, different inbred mouse strains (FVB/N, NZB, PL/J) and one of eight CC founder mouse strains, NZO/H1Lt, when given Cl 13, surprisingly generated robust CTL responses that occurred in the presence of high titers of virus, high PD-1 and Lag3 markers, and high type 1 IFN levels. In addition, these mice died from a fatal immunologic-mediated disease by 7 to 9 d post-Cl 13 infection. Death was due to leakage of exudate into the lung that compromised respiration. The underlying mechanism was replication of virus in pulmonary endothelial cells combined with CTL destruction of such cells. The resultant enhanced vascular permeability was followed by leakage of fluids and cells into the lung, leading to distortion and destruction of pulmonary alveolar air spaces, causing acute respiratory failure and death. Immunopathologic injury and

Significance

T cell exhaustion and successful therapy to restore T cell function initially uncovered with lymphocytic choriomeningitis virus (LCMV) Clone (Cl) 13 infection is important for understanding and treating persistent viral infections and cancers in mice and humans. Here, we report that Cl 13 infection in multiple inbred mouse strains elicits opposite phenotypes: acute death in 7 to 9 d associated with a robust T cell response contrasted to suppression of T cell response leading to persistent infection with normal life span. Death was due to pulmonary vascular leakage of fluids and cells into the lung, leading to respiratory failure. Death can be aborted by blocking interferon-1 signaling or deleting CD8 T cells.

Author contributions: M.B.A.O., Z.M.R., and B.M.S. designed research; B.C.W., L.E.H., M.J.W., R.A., A.Z., and B.M.S. performed research; R.A. contributed new reagents/analytic tools; M.B.A.O., B.C.W., R.A., Z.M.R., and B.M.S. analyzed data; and M.B.A.O. and Z.M.R. wrote the paper.

Reviewers: R.S.B., University of North Carolina at Chapel Hill; and A.J.Z., University of Alabama at Birmingham.

The authors declare no conflict of interest.

[1]To whom correspondence should be addressed. Email: mbaobo@scripps.edu.

This article contains supporting information online at www.pnas.org/lookup/suppl/doi:10.1073/pnas.1804674115/-/DCSupplemental.

Published online July 30, 2018.

death were aborted by blockage of IFN-1 signaling or deletion of CD8 T cells.

Results and Discussion

We obtained inbred murine strains FVB/N (H-2q), SWR/J (H-2q), NZB (H-2d), BALB/c (H-2d), C57BL/6 (H-2b), PL/J (H-2u), SJL/J (H-2s), and C3H (H-2k) from The Jackson Laboratory or The Scripps Research Institute (TSRI) vivarium. When groups of four to six 7- to 8-wk-old males and females from each strain were injected with 2×10^6 pfu of Cl 13 i.v., SWR/J, BALB/cjd, C3H, and C57BL/6 mice from both sexes survived, became persistently infected with virus for varying periods of time over 60 d (Fig. 1*A* and *SI Appendix*, Table S1*A*), and had life spans over the 60- to 90-d observation period. However, the same dose and route of Cl 13 into similarly sexed and aged male or female FVB/N, NZB (21), PL/J, or SJL/J mice resulted in death by 7 to 10 d (Fig. 1*A* and *SI Appendix*, Table S1*A*). Before death, these mice surprisingly had high viral titers, had high levels of type 1 IFN (IFN-1), generated robust antiviral CD8 CTLs, and developed pulmonary vascular permeability, leading to marked exudate into the lung and distorted and diminished alveolar air spaces (Fig. 1 *D*, *G*, and *H*, Table 1, and *SI Appendix*, Table S1*B*: data shown for FVB/N). Death in FVB/N or NZB mice was aborted by blockade of IFN-1 signaling using antibody to IFN-1 receptor (IFNAR) or depleting CD8 T cells (Fig. 1 *A*–*D* and *G*). By contrast,

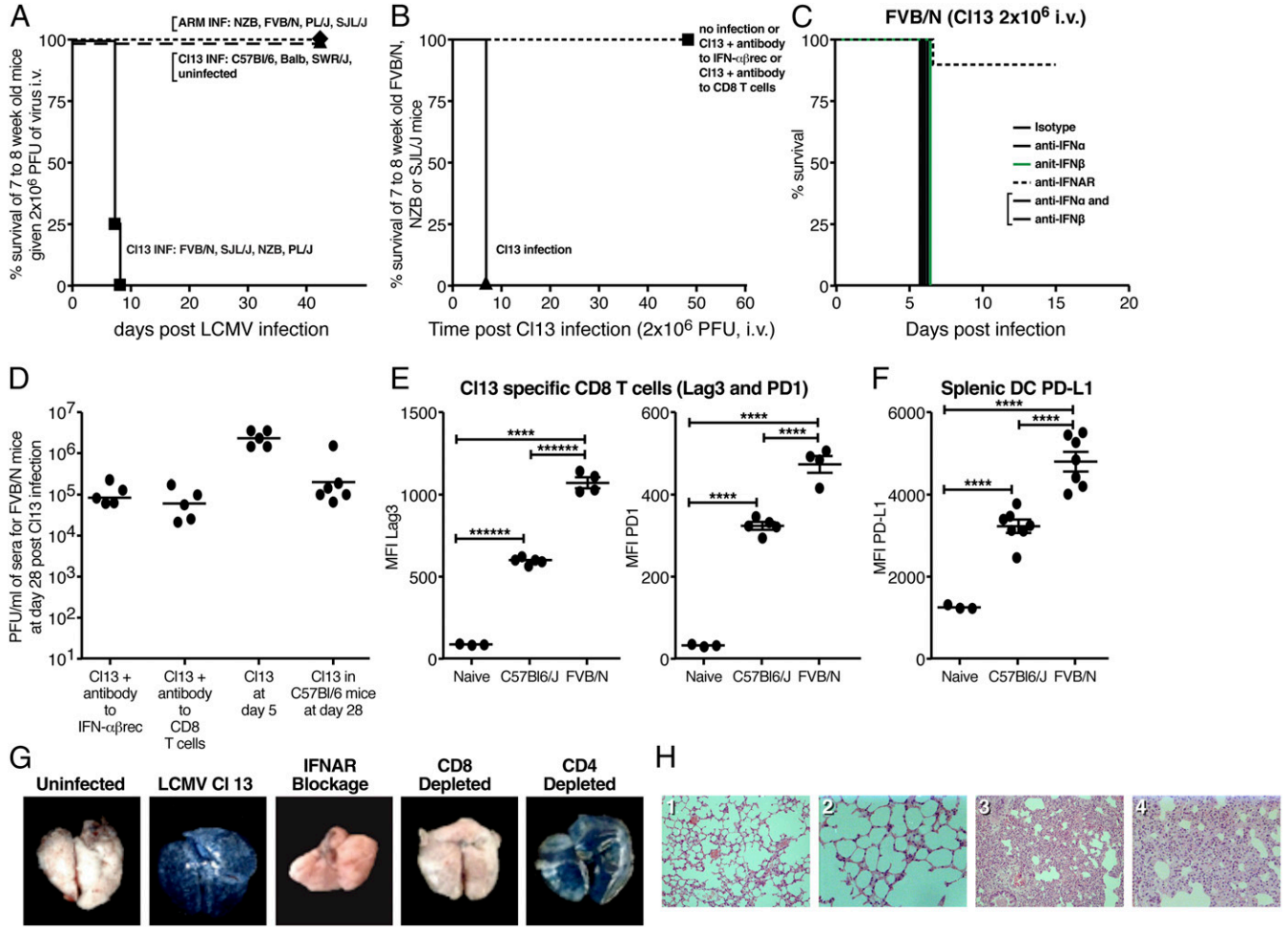

Fig. 1. Occurrence of either acute death or persistent virus infection following Cl 13 infection of different inbred mouse strains. (*A*) FVB/N, SJL/J, NZB, and PL/J mice died 7 to 9 d following i.v. inoculation of 2×10^6 pfu of Cl 13 i.v., but all survived when given 2×10^6 pfu of ARM 53b i.v. By contrast, 100% of C57BL/6, BALB, and SWR/J mice became persistently infected and lived normal life spans following Cl 13 inoculation. (*B*) Cl 13-induced death of FVB/N and NZB mice was aborted by blockage of IFN-1 signaling or deletion of CD8 T cells. (*C*) Antibody to IFNAR prevents the lethal disease caused by Cl 13, but blockade of either IFN1-α 1, 4, 5, 11, 13 or -β separately or combined does not. (*D*) High viral titers in the blood of FVB/N mice 28 d after given Cl 13 when IFN-1 signaling was blocked or CD8 T cells were deleted. In the absence of these treatments, mice died by day 7 to 9 and had viral titers of 6×10^5 to 1×10^6 pfu/mL of blood at day five postreceiving Cl 13. Cl 13 infection of C57BL/6 mice resulted in high levels of virus when sampled at day 28. Similar dose and administration of ARM 53b into FVB/N mice resulted in clearance of virus. Dots record values of individual mice. (*E*) Significant expression ($P \leq 0.001$) of PD-1 and Lag3 on surface of Cl 13-specific CD8 T cells (tetramer selection by immunodominant CD8 T cell epitope) in FVB/N mice (robust T cell response with immune-mediated death) and C57BL/6 mice (T cell exhaustion and persistent infection). Age- and sex-matched mice were used and given 2×10^6 pfu of Cl 13 i.v. Five days after infection, tetramer positive FVB/N cells (NP 118 to 126) and C57BL/6 cells (GP 33 to 41) were harvested and studied by FACS. In addition, concentration of PD-1 and Lag3 molecules on the surface of FVB/N CD8 T cells was significantly ($P \leq 0.001$) more than numbers of similar molecules on surfaces of C57BL/6 tetramer positive CD8 T cells. Each dot records value for an individual mouse. (*F*) PD-L1 expression is significantly elevated ($P \leq 0.001$) on the surface of splenic DCs obtained from both C57BL/6 and FVB/N at day 5 post-Cl 13 infection compared with naive mice. Significant difference ($P < 0.001$) between higher expression on FVB/N infected compared with C57BL/6-infected mice. (*G*) Expression of Evans blue in lungs of FVB/N mice. (*Left* to *Right*) The first panel shows uninfected; the rest of the panels show infected with Cl 13 and manipulated by blocking IFN-1 signaling or deletion of CD8 or CD4 T cells. (*H*, *Left* to *Right*) FVB/N. (*1*) Uninfected lung at 200× magnification; (*2*) uninfected lung at 400× magnification; (*3*) Cl 13-infected lung at day 6, 200× magnification; (*4*) Cl 13-infected lung at day 6, 400× magnification.

Table 1. Survival, IFN-1α,β levels, and virus titer of the eight founder CC mice infected with Cl 13 2×10^6 pfu/mL i.v

Mice	Survival, d PI	IFN-1 (24 h PI)		Viral titer, pfu/mL plasma				
		IFN-α, ng	IFN-β, pg	5*	15*	30*	45*	60*
CC founder								
C57BL/6	>60	61	540	8×10^5	1×10^5	7×10^4	2×10^3	Nil
A/J	>60	19	1,150	6×10^5	1×10^5	7×10^3	8×10^2	Nil
129S1/SvImJ	>60	36	2,016	4×10^5	2×10^4	6×10^3	9×10^2	8×10^2
NOD/LtJ	>60	23	526	2×10^5	2×10^5	2×10^4	7×10^3	$8 \times 10^{3\dagger}$
CAST/EiJ	>60	9	179	9×10^4	8×10^4	3×10^2	7×10^2	Nil
WSB/EiJ	>60	29	196	8×10^5	6×10^4	2×10^4	2×10^3	3×10^3
PWK/PhJ	>60	22	354	2×10^5	2×10^3	Nil	Nil	Nil
NZO/H1Lt	<7	56	1,267	1×10^6	Dead	—	—	—
Control								
FVB/N	<8	55	1,604	1×10^6	Dead	—	—	—

*Days PI.

†NODs' titer at day 90 post Cl 13 infection was 6×10^3 pfu/mL plasma. Four to six mice per group. The pfu values indicate the mean for each group of four to five mice. —, mice dead.

blocking either IFN1-α 1, 4, 5, 11, or 13, or IFN-β separately, or with both antibodies combined did not prevent the acute death (Fig. 1 *C* and *G*). Thus, either to block IFNAR signaling also required antibodies to the other seven missing IFN-1α molecules or the concentration available of the combined antibodies used was not sufficient to block IFNAR signaling. Deleting CD4 T cells did not prevent pulmonary exudate or death (Fig. 1*G*). By contrast, injection of LCMV Armstrong (ARM) 53b virus, 2×10^6 pfu i.v., did not kill FVB/N or NZB strains (Fig. 1*A*). At day 5 to 6 post-Cl 13 challenge, FVB/N (Fig. 1*D*) and NZB mice displayed viral titers of 2×10^5 to 5×10^6 pfu/mL plasma. PD-1 and Lag3 molecules were significantly ($P < 0.001$) enhanced on LCMV-specific CD8 T cells

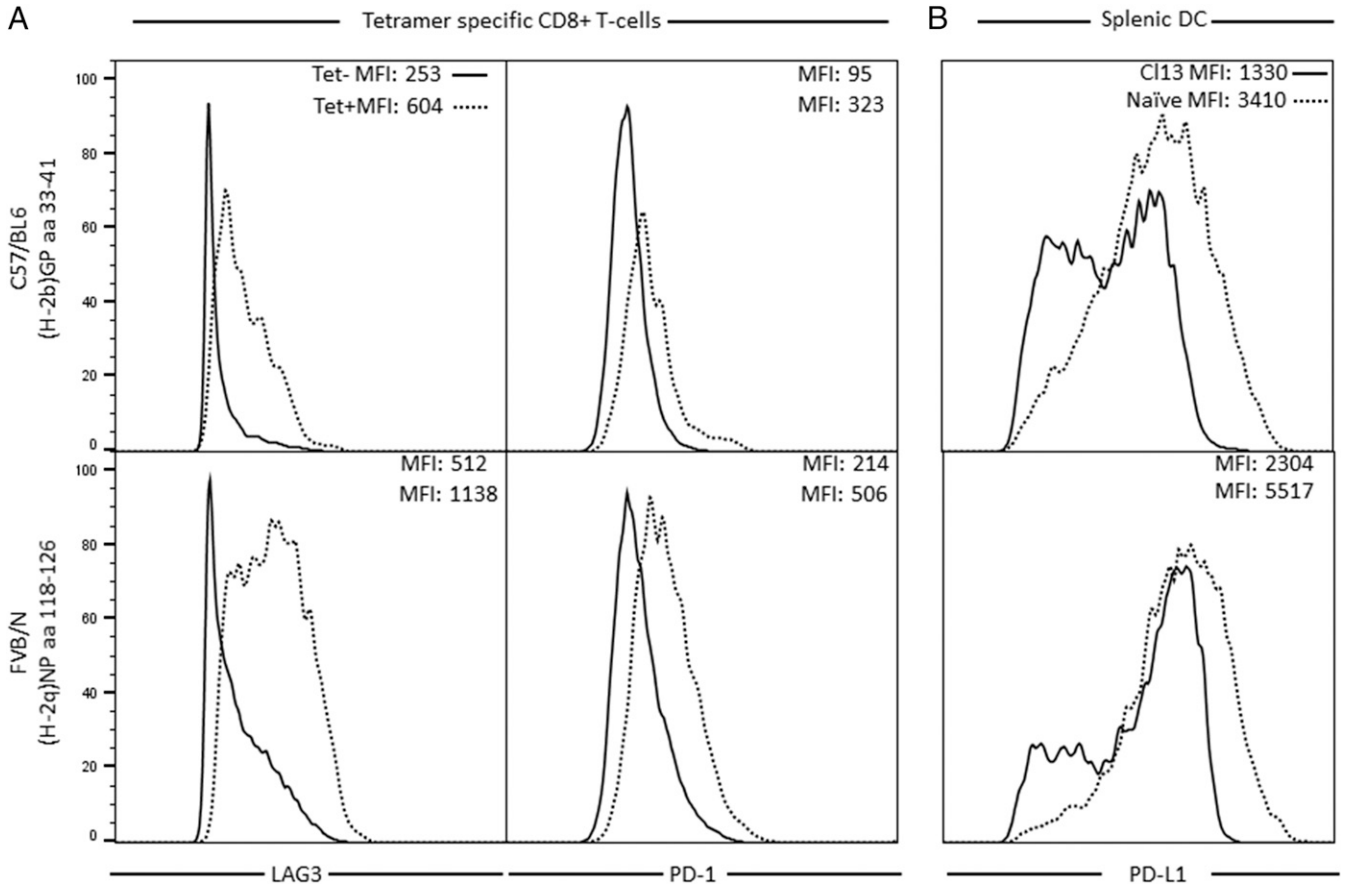

Fig. 2. FACS plots for data summarized in Fig. 1 *E* and *F*. (*A*) Mean fluorescence intensity (MFI) of PD-1 and Lag3 molecules on the surfaces of tetramer-specific $CD8^+$ T cells from C57BL/6 (CTL epitope GP 33 to 41) and FVB/N (CTL epitope NP amino acids 118 to 126) mice 5 d following challenge with 2×10^6 pfu of Cl 13 i.v. (*B*) FACS plots specific for PD-L1 molecules on surfaces of conventional dendritic cells (cDCs) of C57BL/6 and FVB/N mice 5 d following challenge with 2×10^6 pfu of Cl 13 i.v. Each panel records data from a different individual mouse and reflects the response observed routinely in a group of 4 to 5 mice.

and PD-L1 and Lag3 on $CD19^-$, $CD3^-$, B220-, and $CD11c^+$ splenic dendritic cells (DCs) in both C57BL/6 and FVB/N mice 5 d after challenge with Cl 13 compared with naive mice (Figs. 1 *E* and *F* and 2). Interestingly, PD-1 and Lag3 expression was significantly ($P < 0.001$) greater on FVB/N than C57BL/6 virus-specific CD8 T cells and correspondingly on DCs (Figs. 1 *E* and *F* and 2). When antibodies to Lag3 or PD-L1 were used on FVB/N mice infected with Cl 13, 2×10^6 i.v., seven of seven died at day 5. Similar virus inoculated FVB/N mice that were not treated with antibodies died at day 7 to 9. Enhanced CTL activity was associated with 1.5 to 2 logs lower viral titers in the lung and sera. Early injury to the lung and death occurred (seven of seven mice day 5) in these mice compared with mice not treated with antibodies to PD-1 and Lag3 (seven of seven mice at day 7 to 9). C57BL/6 and FVB/N mice infected with Cl 13 had similar and high viral titers (Fig. 1*D*) but dramatically different outcomes (Fig. 1 *A* and *B*). ARM 53b has identical CTL epitopes to Cl 13, but inoculation into adult immunocompetent FVB/N or NZB mice, as well as C57BL/6, BALB, or SWR/J, leads to generation of $CD8^+$ and $CD4^+$ viral-specific T cells and clearance of virus by 10 to 15 d postinfection (PI) and a normal life span. The Cl 13 virus was derived from ARM 53b (8, 9) and differs from ARM 53b by 3 out of 3,356 amino acids, of which only two different residues, one on the glycoprotein residue 260 and one on polymerase at position 1079, play a role in either persistence (Cl 13) or clearance of acute infection (ARM 53b) (22–27). Cl 13 amino acid on the spike glycoprotein (GP) at residue 260 contains a leucine that binds Cl 13 to its cell receptor alpha-dystroglycan (α-DG) (26–30). ARM 53b contains a bulky phenylalanine at this position and binds negligibly to α-DG (26, 27, 29, 30). The other amino acid difference is in the viral polymerase where Cl 13 glutamine at position 1079 favors viral transcription and replication of virus for 1.5 to 2 logs over ARM 53b that contains a lysine at the same residue (23, 25).

Different responses of the inbred mouse strains to Cl 13 infection were not H-2–linked. FVB/N H-2q mice succumbed by day 7 to 8 while H-2q SWR/J mice became persistently infected for over 60 d and lived a normal life span. Similarly, NZB mice (H-2d) died 7 to 9 d post-Cl 13 infection while, in contrast, H-2d BALB infected with Cl 13 became persistently infected for over 60 d and lived approximately 2 y (21). F1s obtained by crossing mice resistant to death (C57BL/6) with mice susceptible to death (FVB/N) resulted in all F1 progeny (seven of seven) dying at 7 to 10 d following Cl 13 challenge (*SI Appendix*, Table S1*A*). This indicated dominance of the lethal phenotype. Two $\times 10^6$ pfu of Cl 13 administered i.v. to backcrosses between F1 (FVB/N × C57BL/6) × C57BL/6 or × FVB/N resulted in four of ten C57BL/6 or nine of ten FVB/N progeny dying over a 15-d observation period (*SI Appendix*, Table S1*A*). Similar results were obtained with F1 (C57BL/6 × NZB) × C57BL/6 or NZB mice. These findings suggest that lethality may be due to a limited number of genes. However, because of the complexity of single-nucleotide polymorphism (SNP) analysis for genome mapping [comparing H-2q mice (FVB/N with SWR/J) or H-2d mice (NZB with BALB)] (*SI Appendix*, Fig. S1), we turned our attention to the eight founder strains of Collaborative Cross (CC) mice (17, 18) to determine if phenotypes of acute death segregated from a persistent infection phenotype. CC founder mice have been sequenced and represent 90% of mus musculus genome variation. If different phenotypes were to occur among these founder CC strains with LCMV Cl 13 infection, these different phenotypes might provide the opportunity to map distinct novel genetic loci and genes involved in T cell exhaustion and restoration of T cell activity.

Using acute death or persistent infection as the phenotypic marker, we inoculated 2×10^6 pfu of Cl 13 i.v. into eight founder CC mouse strains (A/J, 129S1Sv/ImJ, C57BL/6J, CAST/EiJ, WSB/EiJ, NOD/ShiLtJ, PWK/PhJ, and NZO/H1Lt) obtained from The Jackson Laboratory. Seven- to 8-wk-old male or female mice in groups of at least 4 to 5 mice were injected with Cl 13 along with a group of C57BL/6 or BALB (negative control, persistent infection, normal life spans) and FVB/N (positive control, death 7 to 9 d postinoculation) mice. By day 7 to 9, all NZO mice inoculated with 2×10^6 pfu of Cl 13 i.v. died. They had high virus and IFN-1 titers before their death (Table 1). In contrast, the other seven CC founder strains survived Cl 13 infection, lived for over 90 d observation time, and harbored infectious virus for different lengths of time (Table 1, *SI Appendix*, Table S1, and Fig. 3*A*). For example, PWK/PhJ mice were persistently infected for between 15 and 30 d, showing no viremia by day 30, while NOD/ShiLtJ mice still harbored virus over 90 d (Table 1) following Cl 13 infection. NZO mice inoculated with 2×10^6 pfu of ARM 53b all generated antiviral CD8 T cell responses, cleared virus, survived, and lived normal life spans. Owing to the ease of breeding nonobese diabetic (NOD) and FVB/N mice coupled with the autoimmune diseases associated with NOD mice due to robust T cell responses (31–33), we selected NODs as negative and FVB/Ns as positive controls for CC studies. The ability of Cl 13 to kill 100% of NZO mice was totally prevented by either use of antibody to IFNAR to abort IFN-1 signaling or by depletion of CD8 T cells with antibody (Fig. 3*B*). Both susceptible NZO and FVB/N mice had significantly higher levels of type 1 IFN-α or -β following Cl 13 infection than the resistant NOD mice (Fig. 3 *C* and *D*). While depletion of NZO CD8 T cells completely prevented the acute death phenotype (Fig. 3), depletion of CD4 T cells protected only 20% of mice ($P < 0.001$) (Fig. 3*E*). From these experiments, it is clear that action of CD8 T cells and levels of IFN-1 α and β are markers associated with Cl 13-induced acute death of NZO CC mice. Death is dependent on CD8 T cells and IFN-1 signaling.

The next series of studies focused on the pathogenesis for NZO mouse death. Intravenous infection (2×10^6 pfu) of LCMV ARM into NZO mice resulted in the generation of antiviral CTLs that cleared virus and did not kill NZO mice (Fig. 3*A*). By contrast, injection of the same dose and same route of Cl 13 was lethal to NZO within 7 to 9 d (Fig. 3*A*). Cl 13 uses α-DG as its major receptor while ARM does not (28–30). Alpha-DG is located on endothelial cells (30), and Cl 13 virus binds by 1.5 to 2 logs greater affinity to α-DG than does ARM virus (26, 27, 29, 30). Using flow cytometry, we identified pulmonary endothelial cells using antibody to CD31 (21) and analyzed for Cl 13 or ARM expression in these cells from infected NZO mice using an antibody-to-virus nucleoprotein (VL4). As seen in Fig. 4*A*, 3 d post-Cl 13 or ARM infections, expression of viral antigen was negligible in pulmonary endothelial cells. However, by 5 d postinfection, pulmonary endothelial cells from Cl 13-infected NZO mice displayed significantly higher expression of viral antigen compared with pulmonary endothelial cells purified from ARM-infected NZO mice. ARM 53b infection showed the same negligible expression of viral antigen at day 5, mirroring levels observed at day 3 postinfection (Fig. 4*A*). The H-2 type of NZO mice is not known. To perform a virus-specific T cell assay, we modified the in vivo protocol of Liu and Whitton (34). Briefly, 5 d after i.v. administration of either Cl 13 or ARM 53b 2×10^6 pfu, NZO mice and naive control NZO mice were injected i.v. with 180 μg of brefeldin A (BFA). After 6 h of in vivo stimulation with these viruses, spleens and lungs were removed, single cell suspensions were made, and intact cells were stained with antibodies to mark surface expression of CD8, CD4, and B cells, followed by permeabilization of cells and staining with antibodies for intracellular cytokines IFN-γ and TNF-α and analysis by flow cytometry. As shown for lung tissue in Fig. 4*A*, negligible virus-specific CD8 CTL recruitment or activity occurred in lungs of either ARM 53b or Cl 13 infection 3 d postinfection as measured by intracellular cytokine labeling. These results were similar to lack of expression for viral antigen in pulmonary endothelial cells at that time. However, significant expression of intracellular cytokines of isolated virus-specific CD8 CTL in lungs following Cl

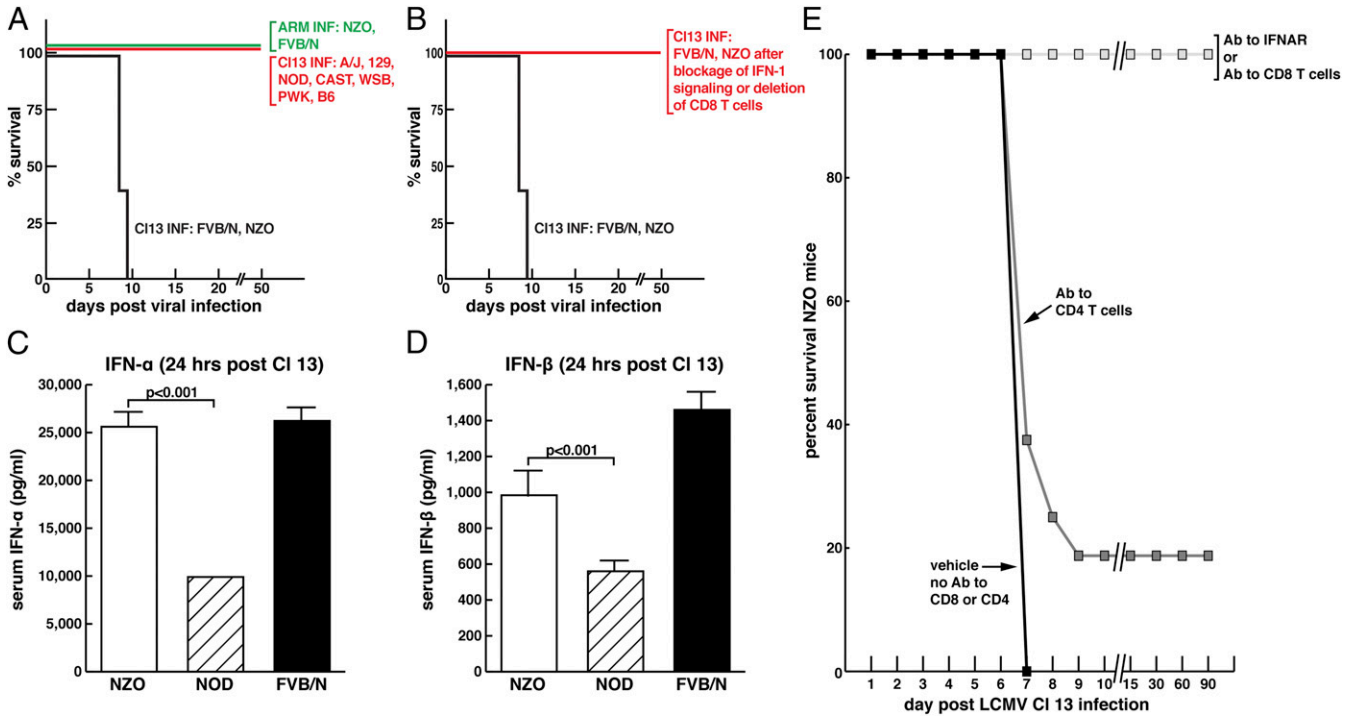

Fig. 3. Occurrence of either acute death or persistent virus infection following Cl 13 infection of founder CC mice. (*A*) Only NZO CC founder mice died following i.v. inoculation of 2×10^6 pfu of Cl 13 i.v. while all other CC founders A/J, 129S1Sv/ImJ, NOD/LtJ, CAST/EiJ, WSB/EiJ, PWK/PhJ, and C57BL/6 (B6) survived and became persistently infected. NZO CC mice did not die from an equivalent dose or route of infection with ARM 53b, lived normal life spans, and cleared virus. (*B*) NZO CC founder mice survived Cl 13 infection if their IFN-1 signaling was blocked or CD8 T cells deleted. (*C*) NZO CC founder mice generated significantly more IFN-1α than NOD CC founder mice 24 h post-Cl 13 i.v. administration. (*D*) NZO CC founder mice generated significantly more IFN-1β than NOD CC mice 24 h post-Cl 13 i.v. administration. (*E*) Blocking IFN-1 signaling or deleted CD8 T cells from NZO mice prevented their death; deletion of CD4 T cells did not.

13 infection occurred by day 5 postinfection, paralleling enhanced expression of viral antigen in pulmonary endothelial cells (Fig. 4*A*). Of interest was the higher amounts of TNF-α compared with IFN-γ in the virus-specific lung CD8 T cells. High TNF-α levels correlated with abundant numbers of polymorphonuclear cells in the lung exudate (Fig. 4 *B*, *Lower*). By contrast, negligible recruitment or expressing of virus-specific CD8 T cell activity occurred at day 5 post-ARM infection (Fig. 4*A*). When Cl 13-infected NZO mice were perfused with Evans Blue on day 6 postinfection, usually 1 or 2 d before their death, marked expression of dye appeared in lungs of Cl 13-infected NZO mice (Fig. 4*B*), but not in either uninfected NZO controls (Fig. 4*B*) or ARM-infected NZO mice. Histologic examination of lungs from NZO mice infected with Cl 13 displayed enhanced vascular permeability, cellular infiltration, and the complete collapse of alveoli (Fig. 4 *B*, *Lower*). Cellular infiltrates were comprised mainly of T cells, clusters of polymorphonuclear cells, monocytes, macrophages, and some plasma cells (Fig. 4 *B*, *Lower*). Study of other tissues indicated modest cellular infiltration into the glomeruli and tubules of the kidney and into the liver (*SI Appendix*, Fig. S2). Disorganization of splenic architecture was also observed with Cl 13 infection (*SI Appendix*, Fig. S2).

Platelets are essential to maintain vascular integrity and arrest bleeding from wounded tissues (35, 36), as well as controlling enhanced vascular permeability during inflammatory reactions (37). Moreover, in mouse models of LCMV ARM infection, platelets control hemorrhage, predominantly cutaneous and from the gastrointestinal tract, which becomes lethal in mice rendered severely thrombocytopenic (38). Of note, the reduction in platelet count resulting from bone marrow dysfunction during LCMV ARM infection, often nearly one log, is not sufficient to cause bleeding as only animals treated with anti-platelet antibody, reducing the platelet count by nearly three logs, developed lethal hemorrhage. This is in agreement with human data showing that the bleeding time test of platelet number and function starts prolonging when that platelet count is 10,000 per μL and is then proportional to the number of platelets between 0 and 10,000 (35, 36). We next asked if Cl 13-induced pulmonary vascular permeability that leads to leakage of fluids and cells into the lung but with minimal evidence of hemorrhage (red blood cells) was related to a drop of platelet numbers and/or platelet dysfunction. As seen in Fig. 5 *A* and *C*, Cl 13 lowered platelet counts in NZO and FVB/N mice by roughly a log but not to levels associated with hemorrhage. These observations, along with anatomic study of lung showing a paucity of red blood cell infiltration (Figs. 1 and 4), support the conclusion that death was likely not due to a viral-induced hemorrhagic disease but rather to virus-induced enhanced vascular permeability. While ARM infection also lowered platelet counts (Fig. 5 *B* and *C*), in some instances by nearly a log at 3 to 6 d postinfection, recovery to normal platelet levels usually occurred by 9 to 12 d postinfection. Platelet levels following Cl 13 infection never rebounded unless either IFN-1 signaling was aborted by treatment with antibody to IFNAR or CD8 T cells were deleted (Fig. 5*A*). The genome of LCMV consists of two RNA segments: a short (S) segment where two genes, the glycoprotein (GP) at the 5′ end and the nucleoprotein (NP) at the 3′ end are placed, and a large (L) segment where the Z gene at the 5′ end and the viral polymerase at the 3′ end are located. The virus GP gene is posttranslationally cleaved to the spike protein (GP1) required to attach to and allow entry into permissive cells and the GP2 transmembrane component. The NP and polymerase comprise the transcription complex, and the Z plays a role in budding. To determine if all genes of Cl 13 were required for the acute death (Figs. 1 and 3, Table 1, and *SI Appendix*, Table S1) and decreased platelet counts (Fig. 5*A*) in FVB/N

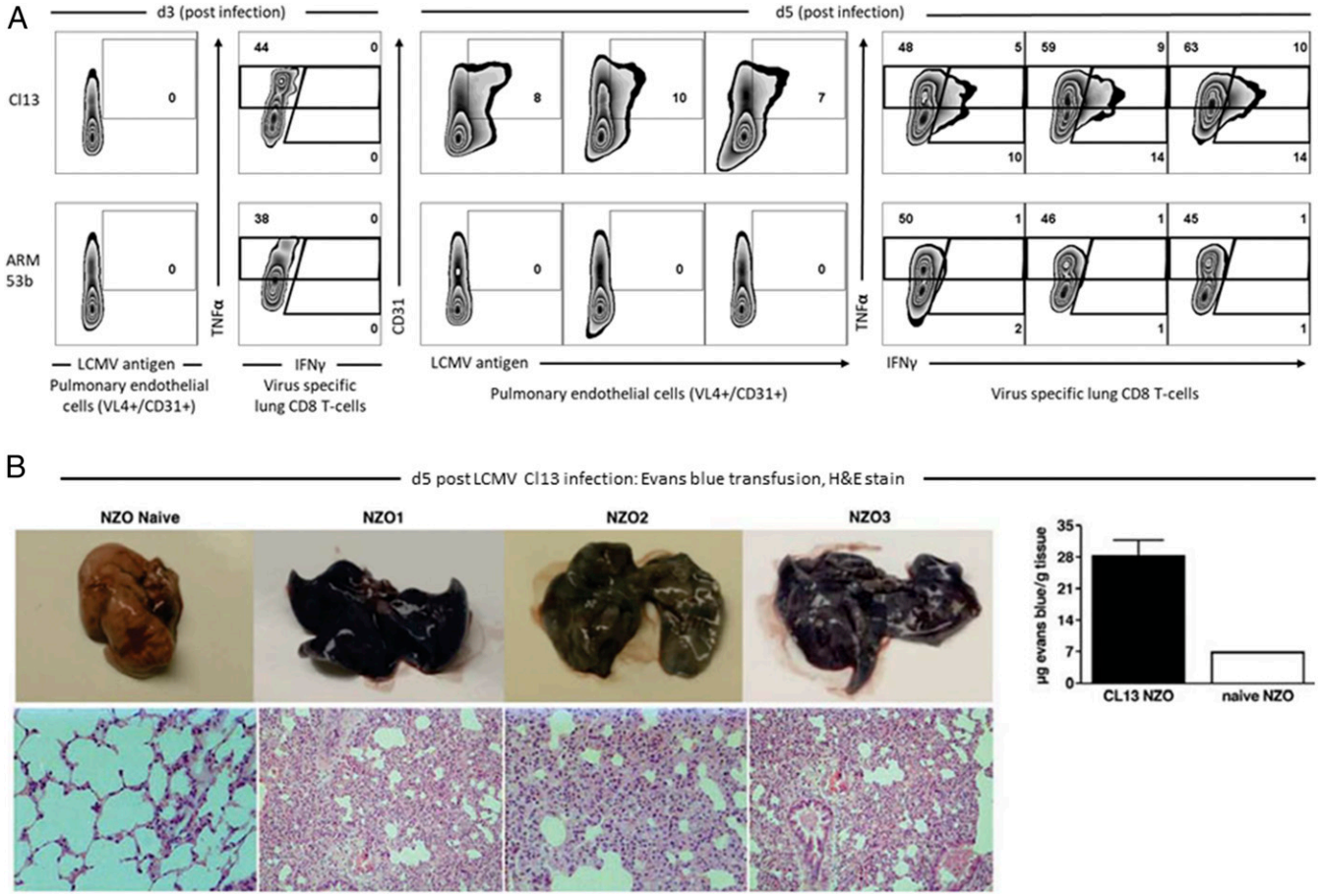

Fig. 4. The pathogenesis of acute death of founder NZO CC mice after Cl 13 infection was due to viral replication in pulmonary endothelial cells, generation of virus-specific CD8 T cells, and their interaction leading to enhanced vascular permeability with exudate into the lung. Consolidation and collapse of alveolar air spaces resulted in respiratory failure. (*A*) At 3 d post-Cl 13 or ARM 53b infection, negligible viral replication in pulmonary endothelial cells or infiltration of virus-specific CD8 T cells into the lung occurred. By day 5 postinfection, the same phenotype of viral antigen expression in pulmonary endothelial cells and migration of virus-specific CD8 T cells into the lungs as witnessed for day 3 was found in NZO mice infected with ARM 53b. In contrast, with Cl 13 inoculation 5 d postinfection, abundant replication of viral antigen in pulmonary endothelial cells occurred with detection of virus-specific CD8 T cells into the lung. (*B*, *Upper*) Leakage of Evans blue in the lung of untreated (naive) or Cl 13-treated (NZO1, NZO2, NZO3) mice. (*B*, *Lower*) The resultant histopathology of mice from each identified group. (*Lower Left* to *Right*) Naive at 400× magnification; NZO1 at 200× magnification; NZO2 at 400× magnification; and NZO3 at 200× magnification.

mice, we made chimeric viruses between Cl 13 and ARM where the S RNA of Cl 13 was matched with the L RNA of ARM and conversely the L RNA of Cl 13 placed with the S RNA of ARM (23, 27, 39, 40). Neither acute vascular permeability and death occurred (zero deaths per seven mice infected with virus containing S RNA Cl 13/L RNA ARM or zero of seven infected with L RNA Cl 13/S RNA ARM) nor did platelet numbers drop to hemorrhagic levels (Fig. 5*B*). These studies indicated that the two amino acid differences encoded by genes of Cl 13 compared with genes of ARM (23, 27, 30) GP1 amino acid 260 Cl 13/ARM Leu/Phe for binding to α-DG the host cell receptor and for entry into permissive endothelial cells and the polymerase amino acid 1079 Gln/Lys important for enhanced transcription and replication were both required for these phenotypes (Figs. 1, 3, and 4*B*). Utilizing chimeric viruses by resorting genes on S RNA or L RNA of Cl 13 with ARM revealed that Cl 13 genes encoded on both the S RNA (GP, NP) or L RNA (Z, polymerase) are required for lethal phenotype in FVB/N mice (Figs. 1, 3, and 5*B*). Sequences of the Cl 13 and ARM viruses are identical for NP and Z, indicating an essential role for Cl 13 GP and L genes in disease causation. These chimeric viruses lowered levels of platelets less than a log and then rebounded toward normal levels. The chimeric virus composed of S RNA of Cl 13 and L RNA of ARM restored platelet numbers significantly slower than infection with chimeric virus S RNA ARM/L RNA Cl 13 over the 18-d observation period (Fig. 5*B*).

As the drop in platelet numbers was not able to explain the observed vascular leakage, we next considered that a defect in platelet function might be involved. The ability of platelets to aggregate is essential for maintenance of vascular barrier function. To test for platelet aggregation function, we mixed platelet-poor plasma (PPP) from vehicle (control)-treated FVB/N mice and from NZO and FVB/N Cl 13-infected mice with platelet-rich plasma (PRP) from untreated animals. Platelets in test and control PRP were treated with 5 μg of ADP to induce aggregation. As shown in Fig. 5*C*, Cl 13 and ARM infection lowered platelet counts to similar levels 3 d postinfection. After that, by day 6, platelet levels dropped in Cl 13-infected NZO mice but rebounded with ARM infection and were restored to pre-infection levels by day 9 postinfection. Fig. 5*D* indicates that, while aggregation was notable throughout the experiment time scale when platelets were mixed with control PPP, in contrast, platelets mixed with PPP from FVB/N or NZO Cl 13-infected mice failed to aggregate. Our findings in FVB/N and NZO mice following Cl 13 infection mirrored our (41) observations and others (42) for Lassa virus (LASV) infections of humans in terms of an inhibitor of platelet aggregation found in plasma. LASV

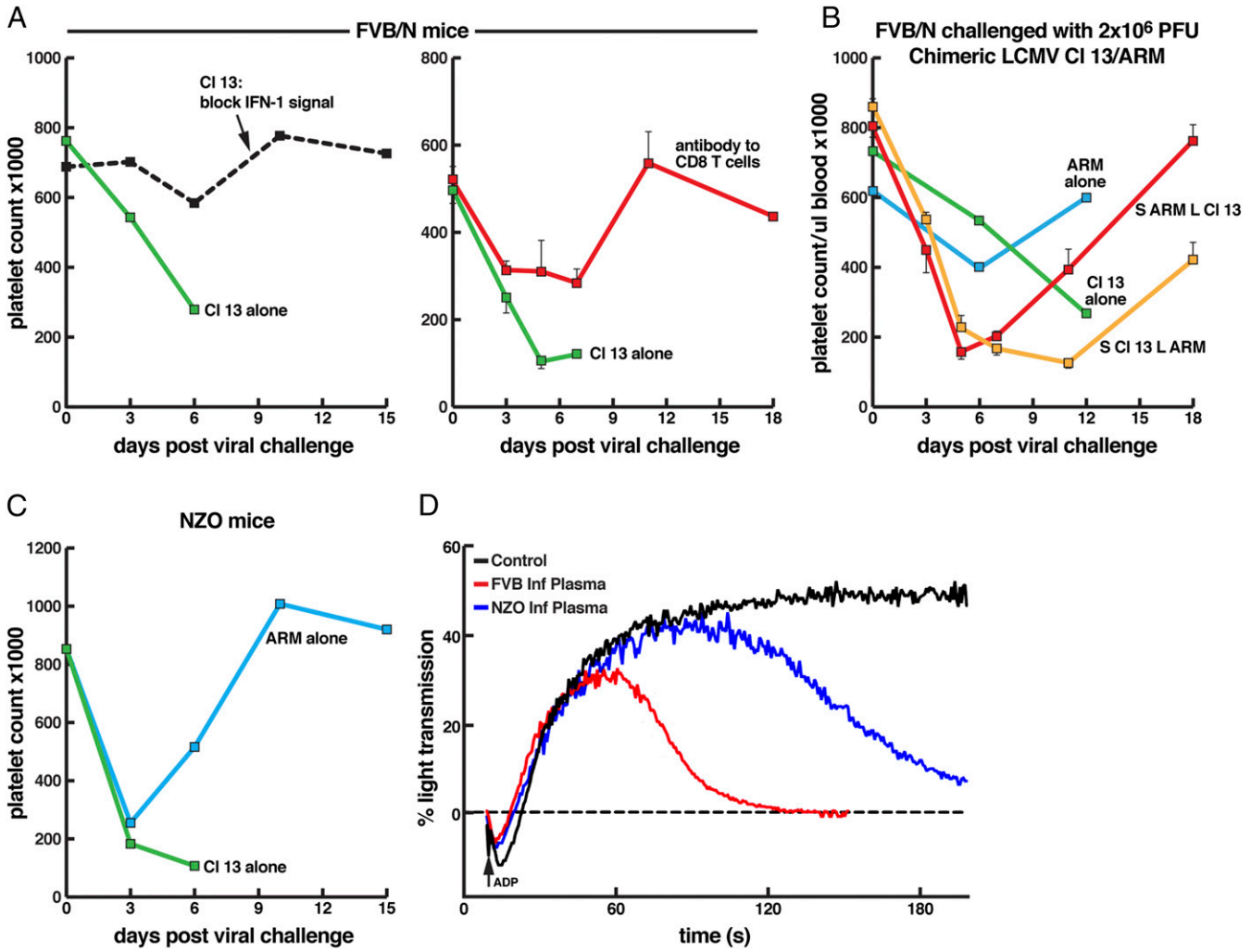

Fig. 5. Platelet counts in FVB/N (*A* and *B*) and NZO CC founder mice (*C*) following 2×10^6 pfu i.v. of either Cl 13 or ARM 53b. (*A–C*) Demonstrated drop in platelet counts in FVB/N and NZO mice following Cl 13 infection. Restoration of platelet counts by blockage of IFN-1 signaling (*A*, *Left*) or deletion of CD8 T cells (*A*, *Right*) are shown. (*B*) Display of the role of chimeric viruses between two segments of LCMV Cl 13 and ARM 53b in effecting platelet count. Two genes, the GP and polymerase, of Cl 13 were required for inability to rebound the low platelet count (orange, S RNA ARM/L RNA Cl 13; red, S RNA Cl 13/LRNA ARM). S RNA of LCMV contains viral genes for GP and NP while the L RNA of LCMV contains the Z and polymerase (L) genes. The sequences of Z and NP of Cl 13 and ARM are identical while the GP and L differ by one amino acid each (23–25, 27, 48). (*D*) Aggregation profile of the plasma inhibitor harvested from FVB/N and NZO mice 5 d post-Cl 13 infection. Plasma was coated on normal platelets and stimulated with ADP, a platelet agonist. Inhibitor of platelet aggregation was found in plasma of Cl 13-infected FVB/N and NZO mice but not in plasma from uninfected mice.

and LCMV are members of the Old World arenaviridae family and share many similarities in structure, cell biology, receptor usage, and CTL activity (43). Presence of a plasma inhibitor of platelet aggregation was not found in ARM-infected FVB/N or NZO mice, nor was it present in mouse strains persistently infected with Cl 13.

Five important points emerged from studies reported here. First, one of serendipity. C57BL/6 mice were selected to explore CTL responses to LCMV Cl 13 and LCMV ARM because of their established genetic and immunologic profiles. Similarly, BALB and SWR/J mice were used for H-2 controls. Results led to findings of T cell kinetics, T cell exhaustion, NIR, and the development of therapeutics to NIR to restore T cell function. However, if different strains like FVB/N, PL/J, or NZB were utilized instead, the scenario of T cell malfunction and restoration would have been replaced by studies of acute death, enhanced vascular permeability, and lung immunopathology. Second, the segregation of NZO CC mice from other CC founder mice and of several non-CC genetically inbred mouse strains as to death or persistent virus outcomes following Cl 13 infection was associated with CD8 T cell generation, high virus titers, high concentration of PD-1 and Lag3 molecules on the surface of virus-specific CD8 T cells, IFN-1 signaling, and platelet abnormalities. Both IFN-1α 1, 4, 5, 11, and 13 and β signaling and Cl 13 genes on the S RNA (glycoprotein) and L RNA (polymerase) are required for the lethal phenotype. Third, the separation of CC founder NZO mice from the other seven founder CC lines using lethality or persistent infection as markers with clear black and white phenotypes following Cl 13 infection should provide a lucid path for mapping genetic loci and genes associated with T cell exhaustion versus a robust T cell response. In addition, CC NZO and inbred FVB/N mice displayed significant differences in IFN-1 signaling levels compared with CC founder NOD mice after Cl 13 challenge. While NZO and FVB/N mice died by 7 to 9 d post-Cl 13 infection, CC NOD mice lived longer life spans, persistently carried virus up to the 90-d period of observation, and developed autoimmune diseases. Fourth, the interaction between pulmonary endothelial cells

expressing LCMV antigen and LCMV-specific CD8 T cells leads to immune-mediated injury. Likely, early events in T cell generation, perhaps related to IFN signaling, modulate different ratios of virus-specific T cells that reacted with different concentration of viral antigens in related cells, like pulmonary endothelial cells, to cause totally different biologic outcomes. One result is excessive immunopathologic injury in FVB/N, NZB, PL/J, and NZO CC mice, leading to death. A different biology may occur when Cl 13 elicited a different ratio of virus-specific T cells in C57BL/6, BALB, SWR/J, and the seven other CC founder mice that led to persistent infection and normal life span. These findings were reminiscent of those of Welsh and coworkers (44, 45), who noted by changing dosage of Cl 13 inoculated into C57BL/6 mice either acute clearance, lethal disease, or persistent infection occurred. As anticipated in FVB/N mice infected with Cl 13, blockage of NIR was associated with high CD8 T cell activity and significantly lower viral titers, exacerbated immunopathologic injury, and an earlier death (day 5, seven of seven mice vs. the expected death at day 7 to 9, seven of seven nonantibody-treated mice).

Fifth, observations on the pathogenesis of the acute lethal disease in CC NZO, as well as inbred FVB/N, NZB, and PL/J mice, are likely to provide insight into human arenavirus disease like that caused by LASV. Cl 13 and LASV have the same dependence on α-DG as the cellular receptor for viral entry (28, 30, 46). Lassa virus in humans and Cl 13 in mice both target primarily endothelial cells, dendritic cells, and macrophages and display a near absence of necrotic injury in tissues they infect (30, 43, 47, 48). NZO, FVB/N, and NZB mice generate viral CTLs following Cl 13 infection, and their interactions with pulmonary endothelial cells that expressed high levels of viral antigens due to possession of cellular receptor, α-DG, led to enhanced vascular permeability, leakage of fluids and cells into the lung. Both LASV infection of humans and infection of NZOs, FVB/N, and NZB mice were accompanied by a log or more drop in circulating platelet counts, but to levels not sufficient to cause hemorrhage (21, 41, 49). However, viral infection likely interfered with the ability of platelets to maintain the integrity of the vascular endothelium by plugging up holes in the vascular endothelium (50), thereby encouraging further enhanced vascular leakage. LASV infection of humans causes defects in platelet aggregation (41, 42, 49) as did Cl 13 infection of NZO and FVB/N mice (Fig. 5). These findings, coupled with anatomic study of injured tissues from LASV and Cl 13 infection, suggest that disease caused by LASV is likely a disease of virus-induced vascular permeability rather than a viral hemorrhagic disease. Research—on platelet signaling, platelet interaction with CTL, IFN-1 signaling, a careful analysis of platelet function in arenavirus infection of mice in appropriately defined strains, and the role of IFN-1 signaling on α-DG, viral entry, and CTL generation, with their relationship to similar studies in humans with LASV infection—should lead to a better understanding of pathogenesis, better diagnostic and therapeutic approaches, and insight into humans infected with LASV and other infections characterized by excessive vascular permeability leading to end organ damage (21, 30, 48, 49, 51).

Materials and Methods

Mice and Viruses. C57BL/6, BALB, SWR/J, NZB, FVB/N, A/J, PL/J, SJL/J, C3H/HeJ, 129S1Sv/lmJ, NOD/LtJ, NZO/H1Lt, CAST/EiJ, PWK/PhJ, and WSB/EiJ mice (6 to 8 wk of age) were obtained from the rodent breeding colony at The Scripps Research Institute (TSRI) or The Jackson Laboratory. All mice were maintained in pathogen-free conditions, and handling conformed to the requirements of the NIH, TSRI Institutional Animal Care and Use Committee, and the American Association for Accreditation of Laboratory Animal Care (AAALAC). LCMV Cl 13 and LCMV ARM 53b were grown, stored, and quantified according to previously published methods (8, 26–28). Mice were infected by i.v. injection of 2×10^6 plaque forming units (pfu) of virus. Both male and female mice were used and were equally susceptible to Cl 13 infection. For quantification of viremia, blood was drawn from the retroorbital sinus under isoflurane anesthesia, serum or plasma was obtained, and viral loads were quantitated by measurement of pfu on Vero E6 cells (9, 26, 28). Tissues (spleen, lung, liver, kidney, heart, and brain) were harvested from euthanized mice and frozen at −80 °C. At time of infectious assay, tissues were thawed, weighed, and homogenized in sterile media (5% FCS) to 10% wt/vol and clarified by low-speed centrifugation, and the resultant supernatant was utilized in plaque assays (9, 26).

Antibody Reagents and Treatments. To abort IFN-1 signaling, mice were treated intraperitoneally (i.p.) with monoclonal antibody to IFN-1 receptor (IFNAR) using antibody MAR1-5A3, IFN-1α with antibody clone TIF-3C5 that blocks only α-1, 4, 5, 11, and 13 or IFN-1β with clone HDβ-4A7 as described (52, 53). For deletion of $CD8^+$ T cells, we used monoclonal antibody YTS169.4, and, for depletion of $CD4^+$ T cells, GK1.5 monoclonal antibody as described (21, 27). Efficiency of $CD8^+$ and $CD4^+$ T cell depletion was >98% as assayed by FACS analysis of blood and spleen cells on day 4. VL4 antibody to LCMV nucleoprotein was purchased from BioXCell and used as reported (53). CD31 antibody was purchased from Biolegend (Clone 390) and used as reported (21). Reagents and procedures used to detect PD-1, PD-L1, AND Lag3 at DCs have been reported (3, 11).

ELISA. Reagents to measure alpha and beta IFN-1 and their analysis were performed as described (52, 53).

Pulmonary Endothelial Studies. Mice were perfused with 10 mL of PBS by cardiac puncture, and lungs were harvested, diced, and suspended in 1 mL of dissociation buffer (1 mg/mL Collagenase D, 100 μg/mL Dnase I) for 30 min at 37 °C. Tissue was processed through 100-μm filters into single cell suspension. Then, 10 mL of Roswell Park Memorial Institute (RPMI)-1640 media was passed through the filters, and material was collected and centrifuged at $500 \times g$ at 4 °C, and decanted, and the collected supernatant was suspended in 1 mL of RBC lysis buffer (150 mM NH_4Cl, 10 mM $KHCO_3$, 100 mM EDTA). After 1 min, 10 mL of cold RPMI buffer was added, and cells were spun at $500 \times g$ at 4 °C, decanted, and resuspended in 1 mL of FACS buffer (2% FBS in 1× PBS). Cells were plated at 1×10^6 cells per well in a 96-well v-bottom plate. Antibodies against CD31-APC (Clone 390; Biolegend), CD45-BV421 (Clone 30F11; Biolegend), CD19-PerCP-Cy5.5 (Clone 6D5; Biolegend), alpha-dystroglycan (α-DG) antibody [Clone IIH6, a gift from Kevin Campbell (University of Iowa School of Medicine)] were diluted 1:200 and added to wells for 1 h at 4 °C, and cells washed and followed by anti-mouse IgM-FITC (Jackson ImmunoResearch) at 1:300 dilution for 30 min at 4 °C. Cells were fixed with 4% paraformaldehyde and gated on $CD45^-$, $CD19^-$, $CD31^+$, and $\alpha\text{-DG}^+$ on an LSR-II (Becton Dickinson). To perform LCMV-antigen staining, all surface staining for pulmonary endothelial cells was done as above without α-DG antibody. The cells were fixed, permeabilized using Cytofix/Cytoperm kit (BD biosciences), and stained with anti-LCMV NP-FITC (Clone VL-4; BioXCell) at 1:400 dilution for 1 h at 4 °C. Samples were gated on $CD45^-$, $CD19^-$, $CD31^+$, and anti-LCMV NP^+ on LSR-II (Becton Dickinson).

Vascular Permeability. Infected and control mice at day 5.5 to 6 postinfection received 200 μL of Evans Blue dye (0.5% in PBS). After 20 min., mice were lethally anesthetized and perfused by intracardiac injection of 10 mL of PBS. Lungs were harvested and photographed, and Evans Blue in the lung was extracted and quantified (21).

Tissue Histology and Cell Isolation. Spleen, lungs, liver, kidneys, heart, and brain were harvested from infected and control mice placed in PBS-buffered formalin and blocked in paraffin, and 10-μm sections were cut and stained with hematoxylin and eosin. Lungs harvested from PBS-perfused mice were initially diced into small pieces for analysis.

FACS. To detect expression of α-DG on or viral antigen expression in pulmonary endothelial cells or CD8 T cells in the lung, we followed procedures of Baccala et al. (21) and Sullivan et al. (27). Isolation and identification of DCs and use of antibody to PD-1 and PD-L1 have been outlined in our publications (11, 26, 29, 52, 53).

In Vivo CTL. We used a modification of the Liu and Whitton method (34). Briefly, NZO mice were infected with LCMV CL 13 or ARM 2×10^6 pfu i.v. Five days later, mice were injected i.v. with 180 μg of BFA in PBS. After 6 h, mice were perfused by cardiac puncture with 10 mL of PBS. Lungs were harvested in cold RPMI, chopped into small chunks, and suspended in 500 μL of dissociation buffer (1 mg/mL Collagenase D, 100 μg/mL Dnase I) on ice for

30 min. Tissue was processed into a single cell suspension by pushing through 100-μm filters. Filters were washed with 10 mL of RPMI, and the suspension was collected and centrifuged at 500 × *g* at 4 °C. The resultant supernatant was decanted and resuspended in 1 mL of RBC lysis buffer (150 mM NH_4Cl, 10 mM $KHCO_3$, 100 mM EDTA) for 1 min. Thereafter, 10 mL of cold RPMI buffer was added, cells were spun at 500 × *g* at 4 °C, supernatant was decanted, and cells were resuspended in 1 mL of FACS buffer (2% FBS in 1× PBS). Spleen and lung samples were stained with CD8-APC/Fire750 (Clone 53-6.7; BioLegend), CD4-PerCP-Cy5.5 (Clone GK1.5; BioLegend), and B220-FITC (Clone RA3-6B2; BioLegend) at 1:200 dilution for 1 h at 4 °C, fixed, and permeabilized using a Cytofix/Cytoperm kit (BD Biosciences). Samples were then stained with TNFα-BV421 (Clone MP6-XT22; BioLegend), IFNg-PE (Clone XMG1.2; BioLegend), and IL-2-APC (Clone JES6-5H4; BioLegend), diluted 1:400 for 18 h at 4 °C. Samples were gated on $CD8^+$, $B220^-$, $CD4^+$, $TNF\alpha^+$, and $IFN\gamma^+$ on an LSR-II (Becton Dickinson). The ^{51}chromium assay has been reported in our publications (26, 53).

Platelet Studies. Blood (0.5 to 1 mL) was collected from the retroorbital plexus into a 1.5-mL capillary tube containing 200 μL of Tris-buffered saline (TBS)/heparin (20 U/mL). Blood was pooled into a 15-mL conical tube with the addition of Tyrode's buffer, pH 7.4 (a 2:5 ratio) and then centrifuged at 100 × *g* for 7 min at room temperature. Platelet-rich plasma (PRP) was removed and stored at room temperature and used within 1 h. Platelet concentrations were measured using an IDEXX ProCyte Dx Hematology Analyzer. Platelet aggregation was performed using a 1:1 mix of infected plasma and uninfected PRP. Platelets were stimulated with 5 μmol/L ADP. Aggregation was assessed using a Chronolog Aggregometer (Model 450) with the Aggrolink software package, version 8 (Chronolog). Aggregation was measured as a maximum percentage of change in transmission of light from baseline, using platelet-poor plasma (PPP) as a reference baseline.

Statistical Analysis. Group comparisons were analyzed by ANOVA in the Prism software package. Experiments were performed in triplicate to ensure reproducibility. $P < 0.05$ was considered significant.

ACKNOWLEDGMENTS. Research was supported by NIH Grants AI009484 and AI099699 (to M.B.A.O.), NIH Grants HL117722 and HL135294 (to Z.M.R.), a Clinical and Translational Science Awards (CTSA) Pilot Award from CTSA Parent Award NIH/National Center for Advancing Translational Sciences (NCATS) Clinical Translational Science Award 5 UL1 TR001114 (to B.M.S.), Medolago Ruggeri (MERU) Foundation (Italy) Fellowships (to A.Z. and R.A.), and Training Grant 5 T32 AI007036 through R. Schooley (University of California, San Diego) (to L.E.H.). Lassa fever samples and studies were funded in part by NIH Contract HHSN272201400048C (to M.B.A.O.). This is Publication 29560 from the Department of Immunology and Microbiology, The Scripps Research Institute.

1. Araki K, Youngblood B, Ahmed R (2013) Programmed cell death 1-directed immunotherapy for enhancing T-cell function. *Cold Spring Harb Symp Quant Biol* 78: 239–247.
2. Pauken KE, Wherry EJ (2015) Overcoming T cell exhaustion in infection and cancer. *Trends Immunol* 36:265–276.
3. Wherry EJ, Kurachi M (2015) Molecular and cellular insights into T cell exhaustion. *Nat Rev Immunol* 15:486–499.
4. Gallimore A, et al. (1998) Induction and exhaustion of lymphocytic choriomeningitis virus-specific cytotoxic T lymphocytes visualized using soluble tetrameric major histocompatibility complex class I-peptide complexes. *J Exp Med* 187:1383–1393.
5. Zajac AJ, et al. (1998) Viral immune evasion due to persistence of activated T cells without effector function. *J Exp Med* 188:2205–2213.
6. Oldstone MBA, Blount P, Southern PJ, Lampert PW (1986) Cytoimmunotherapy for persistent virus infection reveals a unique clearance pattern from the central nervous system. *Nature* 321:239–243.
7. Berger DP, Homann D, Oldstone MBA (2000) Defining parameters for successful immunocytotherapy of persistent viral infection. *Virology* 266:257–263.
8. Ahmed R, Oldstone MBA (1988) Organ-specific selection of viral variants during chronic infection. *J Exp Med* 167:1719–1724.
9. Ahmed R, Salmi A, Butler LD, Chiller JM, Oldstone MBA (1984) Selection of genetic variants of lymphocytic choriomeningitis virus in spleens of persistently infected mice. Role in suppression of cytotoxic T lymphocyte response and viral persistence. *J Exp Med* 160:521–540.
10. Barber DL, et al. (2006) Restoring function in exhausted CD8 T cells during chronic viral infection. *Nature* 439:682–687.
11. Brooks DG, et al. (2008) IL-10 and PD-L1 operate through distinct pathways to suppress T-cell activity during persistent viral infection. *Proc Natl Acad Sci USA* 105: 20428–20433.
12. Brooks DG, et al. (2006) Interleukin-10 determines viral clearance or persistence in vivo. *Nat Med* 12:1301–1309.
13. Ejrnaes M, et al. (2006) Resolution of a chronic viral infection after interleukin-10 receptor blockade. *J Exp Med* 203:2461–2472.
14. Ohaegbulam KC, Assal A, Lazar-Molnar E, Yao Y, Zang X (2015) Human cancer immunotherapy with antibodies to the PD-1 and PD-L1 pathway. *Trends Mol Med* 21: 24–33.
15. Schietinger A, Greenberg PD (2014) Tolerance and exhaustion: Defining mechanisms of T cell dysfunction. *Trends Immunol* 35:51–60.
16. Zarour HM (2016) Reversing T-cell dysfunction and exhaustion in cancer. *Clin Cancer Res* 22:1856–1864.
17. Consortium CC; Collaborative Cross Consortium (2012) The genome architecture of the Collaborative Cross mouse genetic reference population. *Genetics* 190:389–401.
18. Ferris MT, Heise MT (2014) Quantitative genetics in the study of virus-induced disease. *Adv Virus Res* 88:193–225.
19. Morgan AP, et al. (2015) The mouse universal genotyping array: From substrains to subspecies. *G3 (Bethesda)* 6:263–279.
20. Graham JB, et al. (2015) Genetic diversity in the collaborative cross model recapitulates human West Nile virus disease outcomes. *MBio* 6:e00493-15.
21. Baccala R, et al. (2014) Type I interferon is a therapeutic target for virus-induced lethal vascular damage. *Proc Natl Acad Sci USA* 111:8925–8930.
22. Bergthaler A, et al. (2010) Viral replicative capacity is the primary determinant of lymphocytic choriomeningitis virus persistence and immunosuppression. *Proc Natl Acad Sci USA* 107:21641–21646.
23. Lee AM, Cruite J, Welch MJ, Sullivan B, Oldstone MBA (2013) Pathogenesis of Lassa fever virus infection: I. Susceptibility of mice to recombinant Lassa Gp/LCMV chimeric virus. *Virology* 442:114–121.
24. Salvato M, Borrow P, Shimomaye E, Oldstone MBA (1991) Molecular basis of viral persistence: A single amino acid change in the glycoprotein of lymphocytic choriomeningitis virus is associated with suppression of the antiviral cytotoxic T-lymphocyte response and establishment of persistence. *J Virol* 65:1863–1869.
25. Salvato M, Shimomaye E, Oldstone MBA (1989) The primary structure of the lymphocytic choriomeningitis virus L gene encodes a putative RNA polymerase. *Virology* 169:377–384.
26. Sevilla N, et al. (2000) Immunosuppression and resultant viral persistence by specific viral targeting of dendritic cells. *J Exp Med* 192:1249–1260.
27. Sullivan BM, et al. (2011) Point mutation in the glycoprotein of lymphocytic choriomeningitis virus is necessary for receptor binding, dendritic cell infection, and long-term persistence. *Proc Natl Acad Sci USA* 108:2969–2974.
28. Cao W, et al. (1998) Identification of alpha-dystroglycan as a receptor for lymphocytic choriomeningitis virus and Lassa fever virus. *Science* 282:2079–2081.
29. Kunz S, Sevilla N, McGavern DB, Campbell KP, Oldstone MBA (2001) Molecular analysis of the interaction of LCMV with its cellular receptor [alpha]-dystroglycan. *J Cell Biol* 155:301–310.
30. Oldstone MBA, Campbell KP (2011) Decoding arenavirus pathogenesis: Essential roles for alpha-dystroglycan-virus interactions and the immune response. *Virology* 411: 170–179.
31. Bach JF (1992) The Non Obese Diabetic (NOD) mouse, as a model of T cell mediated autoimmune disease. *C R Acad Sci III* 314(Suppl 9):45–46.
32. Ignatius Arokia Doss PM, Roy AP, Wang A, Anderson AC, Rangachari M (2015) The non-obese diabetic mouse strain as a model to study CD8(+) T cell function in relapsing and progressive multiple sclerosis. *Front Immunol* 6:541.
33. Unanue ER, Ferris ST, Carrero JA (2016) The role of islet antigen presenting cells and the presentation of insulin in the initiation of autoimmune diabetes in the NOD mouse. *Immunol Rev* 272:183–201.
34. Liu F, Whitton JL (2005) Cutting edge: Re-evaluating the in vivo cytokine responses of CD8+ T cells during primary and secondary viral infections. *J Immunol* 174: 5936–5940.
35. Weiss HJ (1975a) Platelet physiology and abnormalities of platelet function (first of two parts). *N Engl J Med* 293:531–541.
36. Weiss HJ (1975b) Platelet physiology and abnormalities of platelet function (second of two parts). *N Engl J Med* 293:580–588.
37. Boulaftali Y, et al. (2013) Platelet ITAM signaling is critical for vascular integrity in inflammation. *J Clin Invest* 123:908–916.
38. Iannacone M, et al. (2008) Platelets prevent IFN-alpha/beta-induced lethal hemorrhage promoting CTL-dependent clearance of lymphocytic choriomeningitis virus. *Proc Natl Acad Sci USA* 105:629–634.
39. Emonet SE, Urata S, de la Torre JC (2011) Arenavirus reverse genetics: New approaches for the investigation of arenavirus biology and development of antiviral strategies. *Virology* 411:416–425.
40. Sánchez AB, de la Torre JC (2006) Rescue of the prototypic Arenavirus LCMV entirely from plasmid. *Virology* 350:370–380.
41. Horton LE, et al. (2017) Dysfunctional platelet aggregation in patients with acute Lassa fever. *Open Forum Infect Dis* 4(Suppl 1):S223.
42. Cummins D, et al. (1989) A plasma inhibitor of platelet aggregation in patients with Lassa fever. *Br J Haematol* 72:543–548.
43. Buchmeier MJ, de la Torre JC, Peters CJ (2007) Arenaviridae: The virus and its replication. *Fields Virology*, eds Knipe DM, Howley PM (Williams & Wilkins, Philadelphia), 5th Ed, pp 1791–1828.
44. Cornberg M, et al. (2013) Clonal exhaustion as a mechanism to protect against severe immunopathology and death from an overwhelming CD8 T cell response. *Front Immunol* 4:475.

45. Waggoner SN, Cornberg M, Selin LK, Welsh RM (2011) Natural killer cells act as rheostats modulating antiviral T cells. *Nature* 481:394–398.
46. Spiropoulou CF, Kunz S, Rollin PE, Campbell KP, Oldstone MBA (2002) New World arenavirus clade C, but not clade A and B viruses, utilizes alpha-dystroglycan as its major receptor. *J Virol* 76:5140–5146.
47. Matsumura K, Shasby DM, Campbell KP (1993) Purification of dystrophin-related protein (utrophin) from lung and its identification in pulmonary artery endothelial cells. *FEBS Lett* 326:289–293.
48. Oldstone MBA (2002) Biology and pathogenesis of lymphocytic choriomeningitis virus infection. *Curr Top Microbiol Immunol* 263:83–117.
49. McCormick JB, Fisher-Hoch SP (2002) Lassa fever. *Curr Top Microbiol Immunol* 262:75–109.
50. Guidotti LG, et al. (2015) Immunosurveillance of the liver by intravascular effector CD8(+) T cells. *Cell* 161:486–500.
51. Hara Y, et al. (2011) Like-acetylglucosaminyltransferase (LARGE)-dependent modification of dystroglycan at Thr-317/319 is required for laminin binding and arenavirus infection. *Proc Natl Acad Sci USA* 108:17426–17431.
52. Ng CT, et al. (2015) Blockade of interferon beta, but not interferon alpha, signaling controls persistent viral infection. *Cell Host Microbe* 17:653–661.
53. Teijaro JR, et al. (2013) Persistent LCMV infection is controlled by blockade of type I interferon signaling. *Science* 340:207–211.